AUTHOR(S): IMRAN, M., YOUSAF, A.B., ZAIDI, S.J. and FERNANDEZ, C.

TITLE: Tungsten-molybdenum oxide nanowires/reduced graphene oxide nanocomposite with enhanced and durable performance for electrocatalytic hydrogen evolution reaction.

YEAR: 2017.

Publisher citation: IMRAN, M., YOUSAF, A.B., ZAIDI, S.J. and FERNANDEZ, C. 2017. Tungsten-molybdenum oxide nanowires/reduced graphene oxide nanocomposite with enhanced and durable performance for electrocatalytic hydrogen evolution reaction. International journal of hydrogen energy [online], 42(12), pages 8130-8138. Available from: https://doi.org/10.1016/j.ijhydene.2017.02.152

OpenAIR citation: IMRAN, M., YOUSAF, A.B., ZAIDI, S.J. and FERNANDEZ, C. 2017. Tungsten-molybdenum oxide nanowires/reduced graphene oxide nanocomposite with enhanced and durable performance for electrocatalytic hydrogen evolution reaction. International journal of hydrogen energy, 42 (12), pages 8130-8138. Held on OpenAIR [online]. Available from: https://openair.rgu.ac.uk

INTERNATIONAL JOURNAL OF HYDROGEN ENERGY XXX (2017) 1–9

Available online at www.sciencedirect.com

ScienceDirect

journal homepage: www.elsevier.com/locate/he

Tungsten-molybdenum oxide nanowires/reduced graphene oxide nanocomposite with enhanced and durable performance for electrocatalytic hydrogen evolution reaction

M. Imran [a,*,1], Ammar Bin Yousaf [a,b,1], Syed Javaid Zaidi [b], Carlos Fernandez [c]

[a] Division of Nanomaterials and Chemistry, Hefei National Laboratory for Physical Sciences at Microscale, University of Science and Technology of China, Hefei, Anhui 230026, PR China

[b] Center for Advanced Materials, Qatar University, Doha 2713, Qatar

[c] School of Pharmacy and Life Sciences, Sir Ian Wood Building, Robert Gordon University, AB10 7GJ Aberdeen, UK

ARTICLE INFO

Article history:
Received 25 July 2016
Received in revised form
20 February 2017
Accepted 21 February 2017
Available online xxx

Keywords:
Tungsten-molybdenum oxide
Hydrogen evolution reaction
Reduced graphene oxide
Synergistic effect
Electrocatalysis

ABSTRACT

Hydrogen has attracted huge interest globally as a durable, environmentally safe and renewable fuel. Electrocatalytic hydrogen evolution reaction (HER) is one of the most promising methods for large scale hydrogen production, but the high cost of Pt-based materials which exhibit the highest activity for HER forced researchers to find alternative electro-catalyst. In this study, we report noble metal free a 3D hybrid composite of tungsten-molybdenum oxide and reduced graphene oxide (GO) prepared by a simple one step hydrothermal method for HER. Benefitting from the synergistic effect between tungsten-molybdenum oxide nanowires and reduced graphene oxide, the obtained W-Mo-O/rGO nanocomposite showed excellent electro-catalytic activity for HER with onset potential 50 mV, a Tafel slope of 46 mV decade^{-1} and a large cathodic current, while the tungsten-molybdenum oxide nanowires itself is not as efficient HER catalyst. Additionally, W-Mo-O/rGO composite also demonstrated good durability up to 2000 cycles in acidic medium. The enhanced and durable hydrogen evolution reaction activity stemmed from the synergistic effect broadens noble metal free catalysts for HER and provides an insight into the design and synthesis of low-cost and environment friendly catalysts in electrochemical hydrogen production.

Introduction

Hydrogen, as a durable and renewable clean fuel is a promising energy carrier to address the increasing energy demand of modern world [1]. Recently, researchers have devoted much attention on alternate methods of producing hydrogen as steam reformation of fossil fuels causing increased concerns on earth's climate. Electrochemical water splitting or the hydrogen evolution reaction (HER) for renewable energy has been proposed as the most economic and sustainable

* Corresponding author.
E-mail address: imran345@mail.ustc.edu.cn (M. Imran).
[1] These two authors contributed equally to this work.

http://dx.doi.org/10.1016/j.ijhydene.2017.02.152
0360-3199/

alternate method for large scale hydrogen production [2]. Currently, platinum or Pt-based materials exhibit the highest activity for hydrogen evolution reaction (HER), but their high cost and low abundance limit their large scale applications [3]. Thus, the development of highly efficient and low-cost electrocatalyst for HER still remains a major challenge [4].

Researchers have proposed the use of more economical metals such as, Ni, Mo, W, and other transition metal based electrocatalysts for hydrogen evolution reaction (HER). Nanoparticles of these metals and their inter-metallic compounds [5,6], oxide [7], carbide [8,9], sulfide [10,11] and phosphides [12,13] may replace the expensive Pt catalysts. However, there are a few materials which exhibit satisfied activities for electrocatalytic hydrogen evolution reaction (HER) compared to commercial Pt/C catalyst [14]. Moreover, the synthesis of many high efficiency catalysts for H_2 evolution always involves multiple steps, including precursor synthesis and high-temperature treatment which increases the overall production cost of hydrogen [15]. Mo-based compounds emerged as a new class of electrocatalysts due to its Pt-like catalytic behaviors [16–18]. It has also been observed that mixed phase Mo compounds with other transition metals enhance the activity, as in case of Fe–Ni–P [19,20], Ni–Mo–S [21] and Co–Mo–N [22] which were found to exhibit superior HER performance than the corresponding single component. The synergistic effect of different components may change the surface morphology and intrinsic electric properties of materials to expose more active sites and improve HER activity. The incorporation of the congeneric tungsten (W) element into Molybdenum may play a contributing role, as WO_3 nanoplates prove its potential use in electrocatalysis [23]. Motivated by this strategy, we propose the use of mixed bimetallic alloy of molybdenum with tungsten for hydrogen evolution reaction (HER).

To further enhance the electrochemical performance, a conducting support has been proposed which not only prevent the nanoparticles from agglomeration but also favors the electron transfer during catalytic process [24,25]. Carbon based materials such as graphene oxide, activated carbon and carbon nanotubes (CNTs) have been widely used as support for the design and synthesis of various industrial catalysts [26]. The morphology and nature of carbon materials used as supporting materials for active transition metals generally determine the activities of these catalysts. The large surface area, outstanding electronic conductivity, surface functional groups and improved metal-support interactions are responsible for the significant change in the catalytic performances of supported catalysts [27]. Graphene oxide (GO) has attracted considerable attention due to its excellent chemical stability and fast electron transfer properties compared to the other carbon based materials. The 2D configuration of graphene sheets results in exposure of both sides to the solution which increases active surface area [28,29]. Molybdenum and reduced graphene oxide (rGO) composite materials also proves to be highly active electrocatalysts [30,31]. MoO_2/graphene nanomaterials also showed excellent properties as anode material for Li ion batteries [32]. Herein, we present the design and synthesis of mixed phase tungsten-molybdenum oxide nanowires and reduced graphene oxide nanocomposite by one step hydrothermal method. The synergistic effect of graphene oxide (GO), tungsten-molybdenum oxide nanowires directly enables excellent HER catalytic performance which is comparable with commercial Pt/C catalyst. Our W-Mo-O/rGO catalyst exhibits an enhanced electrocatalytic activity with negligible onset potential and a Tafel slop of 46 mV per decade. Our study demonstrated that the low-cost and easy fabricated W-Mo-O/rGO composite material is a promising candidate as a high efficiency electrochemical hydrogen evolution catalyst.

Experimental

Chemicals

Ammonium molybdate tetrahydrate, $((NH_4)_6Mo_7O_{24}\cdot 4H_2O)$, Sodium nitrate ($NaNO_3$), sodium tungstate dihydrate ($Na_2WO_4\cdot 2H_2O$), Potassium persulfate ($K_2S_2O_8$), Phosphorus pentoxide (P_2O_5), Potassium permanganate ($KMNO_4$), ammonium sulfate ($(NH_4)_2SO_4$) and graphite powder were purchased from Sigma Aldrich and were used as received. All other chemical reagents were of analytical grade and used as received without further purification.

Characterization

The morphology of the particles was observed by scanning electron microscope (SEM, JSM 6700F, JEOL). Transmission electron microscopic (TEM) images and high-resolution transmission electron microscopic (HRTEM) images were carried out on a JEM-2100F field emission electron microscope at an accelerating voltage of 200 kV. The high-angle annular dark-field scanning transmission electron microscopy (HAADF-STEM) image and EDX mapping images were taken on a JEOL JEM-ARF200F atomic resolution analytical microscope. Solid Raman spectra were measured on a Labram-010 micro-Raman spectrometer. The X-ray powder diffraction (XRD) patterns of the products were performed on a Philips X'Pert Pro Super diffractometer with Cu-Kα radiation ($\lambda = 1.54178$ Å). The operation voltage was maintained at 40 kV and current at 200 mA, respectively. The X-ray photoelectron spectroscopy (XPS) was carried out on a PerkinElmer RBD upgraded PHI-5000C ESCA system.

Electrochemical measurements

Before each electrochemical experiment, a glassy carbon (GC) electrode (0.196 cm^2 geometric surface area) was first polished with alumina slurry (Al_2O_3, 0.05 μm) on a polishing mat to obtain a mirror-finish, followed by sonication in 0.1 M HNO_3, 0.1 M H_2SO_4, and DI water for 10 min successively. Then, the catalyst in DI water was drop-coated on to the polished electrode surface using a microliter syringe, which was then dried under vacuum at room temperature. After drying, the catalyst film was covered with a thin layer of Nafion (0.1 wt.% in water, 5 μL) to ensure that the catalyst was tightly attached to the electrode surface during electrochemical measurements. Voltammetry measurements were carried out with a CHI750D electrochemical workstation in a standard three-electrode setup with a working electrode, Ag/AgCl electrode as a

Please cite this article in press as: Imran M, et al., Tungsten-molybdenum oxide nanowires/reduced graphene oxide nanocomposite with enhanced and durable performance for electrocatalytic hydrogen evolution reaction, International Journal of Hydrogen Energy (2017), http://dx.doi.org/10.1016/j.ijhydene.2017.02.152

reference, and platinum wire as a counter electrode. After the measurements, all experimental results were converted with respect to standard RHE reference electrode. To measure the HER activity, 0.1 M $HClO_4$ solution was used. The electrolyte solution was purged and saturated with N_2, in order to create inert atmosphere and avoid the interference due to the presence of dissolved oxygen during electrochemical measurements. Then the catalyst-functionalized GC electrode was immersed in the solution and rotated at 1000 rpm using a rotating disk electrode workstation. Measurements were taken at a 5 mV s^{-1} scan rate by linear sweep voltammetry (LSV). The accelerated durability test for long-term stability of electrodes was investigated by electrochemical cycling in a potential window range between −0.30 and 0.30 versus RHE in 0.1 M $HClO_4$ solution, at a scan rate of 10 mV s^{-1} with 1000 rpm rotation speed for up to 2000 cycles.

Synthesis of graphene oxide

Graphene oxide (GO) was synthesized from graphite powder by modified Hummer's method [33]. In general, graphite powder (4 g) was gradually added into concentrated sulfuric acid solution (H_2SO_4, 24 mL) containing 8 g of $K_2S_2O_8$ and P_2O_5 each at stirred at 80 °C for 6 h. The resulting dark blue mixture was slowly cooled down to room temperature and diluted with 300 mL of H_2O, filtrated and dried in vacuum oven at 60 °C for 12 h. The preoxidized graphite powder (2 g) was then added into H_2SO_4 (92 mL) in ice-bath, then 12 g $KMnO_4$ was gradually added under continuous stirring. After 20 min, sodium nitrate ($NaNO_3$, 2 g) was added into the mixture and solution was further stirred at 30 °C for 2 h and then 200 mL H_2O was added. After being stirred for another 15 min, the reaction was terminated by addition of 560 mL of H_2O and 10 mL of 30% H_2O_2. The product was extensively washed with HCl, water, and then dialyzed to remove acids and residual metal ions. The as-synthesized GO was then dispersed in distilled water at a concentration of 10 mg/mL with the help of sonication.

Synthesis of tungsten-molybdenum oxide nanowires/ reduced graphene oxide nanocomposites

Mixed phase tungsten-molybdenum oxide nanowires/ reduced graphene oxide nanocomposites were synthesized by one step hydrothermal method. Generally, 100 mg of ammonium molybdate tetrahydrate, ($(NH_4)_6Mo_7O_{24}\cdot 4H_2O$) and 92 mg of sodium tungstate dihydrate ($Na_2WO_4\cdot 2H_2O$) were added into 20 mL of DI-water, the pH of the solution was adjusted to ≈3 by adding HCl (1 M), then 50 mg of graphene oxide dispersion was added into the mixture followed by hydrothermal treatment in the autoclave at 180 °C for 12 h. After being cool down to room temperature, the resultant solid was washed several times with DI water and ethanol and dried in vacuum oven overnight at 60 °C for further use. The bare tungsten-molybdenum oxide nanowires were obtained in a similar way except the use of graphene oxide (GO).

Results and discussion

The strategy for the synthesis of hybrid W-Mo-O/rGO composite is illustrated in Fig. 1. For this purpose, we initially synthesized graphene oxide by modified Hummer's method, which introduces a large number of oxygenated functional groups that allow GO to be well dispersed in water (Fig. S1). In the next step, we synthesized W-Mo-O/rGO composites by using ammonium molybdate tetrahydrate and sodium tungstate dihydrate as Molybdenum and tungsten source respectively. The size and morphology of as synthesized W-Mo oxide nanowires and W-Mo-O/rGO composites were observed by scanning electron microscopy (SEM) and transmission electron microscopy (TEM). Fig. 2A shows SEM images of tungsten-molybdenum oxide nanowires, the length of nanowires is in micron and width is about 50 nm. Fig. 2B shows SEM images of the W-Mo-O/rGO composites, graphene oxide surface have been uniformly decorated with tungsten-molybdenum oxide nanowires. The hybrid nanocomposites (W-Mo-O/rGO) comprise interconnected well-defined 3D porous networks with pore sizes ranges from nanometer to several micrometers.

The low magnification TEM images of tungsten-molybdenum oxide nanowires and W-Mo-O/rGO composites are shown in Figs. 2C, D and 3A. The tungsten-molybdenum oxide nanowires are randomly oriented around reduced graphene oxide nanosheets forming a compact, disordered 3D structure. The growth of nanowires on the GO surface may greatly affected by the oxygenated and carboxyl functional groups, which serve as the active sites during the nucleation and growth processes. The intimate contact of the nanowires with reduced graphene oxide was assessed by high resolution transmission electron microscopy (HRTEM). The HRTEM

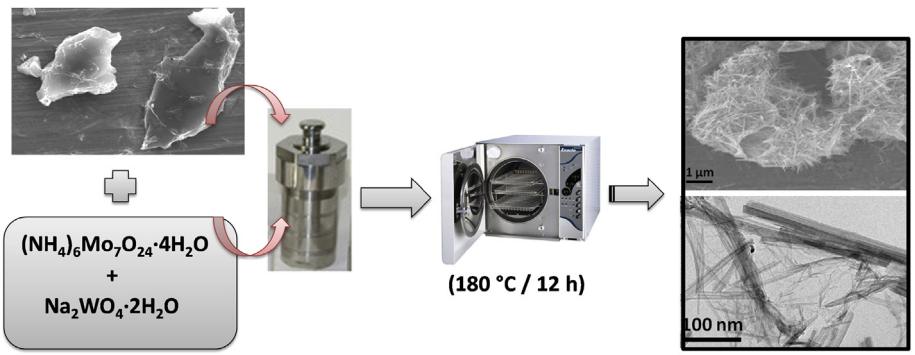

Fig. 1 – Schematic representation for the synthesis of W-Mo-O/rGO nanocomposites.

Please cite this article in press as: Imran M, et al., Tungsten-molybdenum oxide nanowires/reduced graphene oxide nanocomposite with enhanced and durable performance for electrocatalytic hydrogen evolution reaction, International Journal of Hydrogen Energy (2017), http://dx.doi.org/10.1016/j.ijhydene.2017.02.152

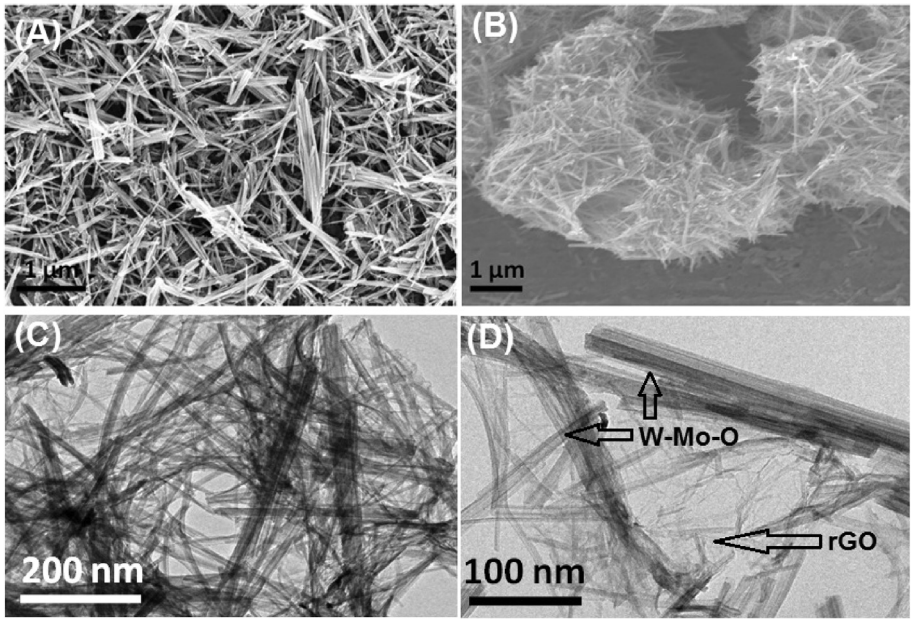

Fig. 2 – SEM images of W-Mo-O nanowires (A) and W-Mo-O/rGO nanocomposite (B), TEM images of W-Mo-O nanowires (C) and W-Mo-O/rGO nanocomposite (D).

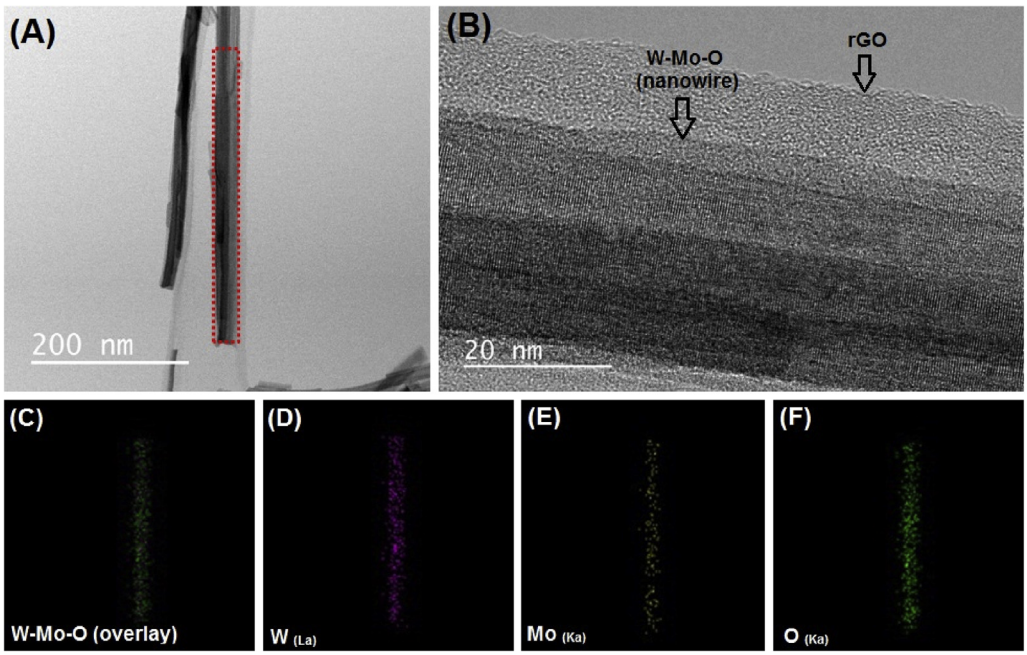

Fig. 3 – TEM image of W-Mo-O/rGO nanocomposite (A), HRTEM image W-Mo-O/rGO nanocomposite (B), HAADF-STEM element mappings of W-Mo-O nanowires (C–F).

images indicate the homogeneous distribution of nanowires over rGO surface comprising a composite material, and the apparent contrast between the W-Mo-O nanowires and the rGO sheet offers an evidence for the formation of hybrid composite (Fig. 3B). In addition, HAADF-STEM element mappings were further performed and it can be clearly seen from Fig. 3C–F that W, Mo and O are evenly distributed, indicating the formation of mixed phase alloy. Energy dispersive X-ray (EDX) spectrum also used to confirm the existence of tungsten molybdenum and oxygen, the atomic ratio of W: Mo was 1:1 which is in agreement with the experimental data as can be seen in Fig. S2.

The XRD spectra of as-synthesized W-Mo-O nanowires and W-Mo-O/rGO were also recorded to determine the purity and crystallinity of the samples. The X-ray diffraction patterns presented in Fig. 4A manifest peaks at $2\theta = 23.3$ (110), 33.7 (111), 46.3 (061) assigned to orthorhombic phase of molybdenum oxide, MoO_3 (JCPDS # 35-0609) with cell parameters

Please cite this article in press as: Imran M, et al., Tungsten-molybdenum oxide nanowires/reduced graphene oxide nanocomposite with enhanced and durable performance for electrocatalytic hydrogen evolution reaction, International Journal of Hydrogen Energy (2017), http://dx.doi.org/10.1016/j.ijhydene.2017.02.152

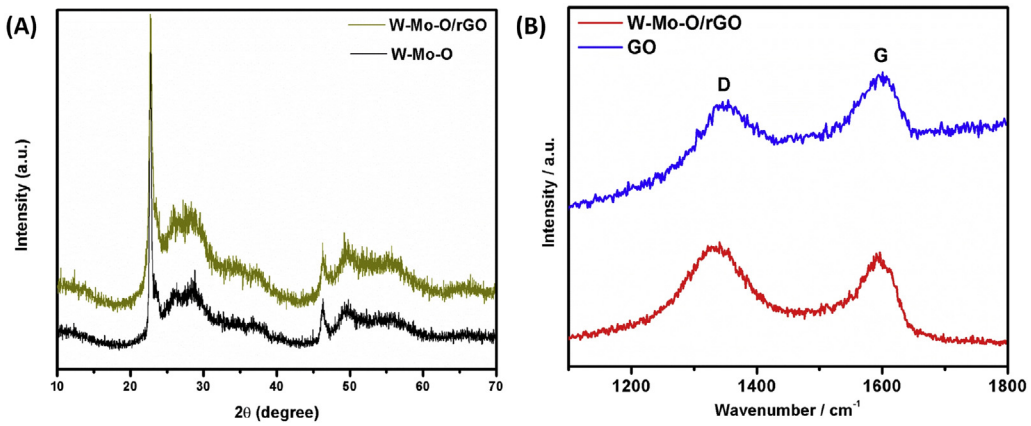

Fig. 4 – XRD pattern of as synthesized W-Mo-O nanowires and W-Mo-O/rGO nanocomposite (A), Raman spectrum of graphene oxide and W-Mo-O/rGO nanocomposite (B).

a = 3.92 Å, b = 13.83 Å, c = 3.66 Å, while additional peaks at 2θ = 22.6 and at 26.2 were also observed for MoO_3 (JCPDS # 09-0209) indicating the presence of mixed phases of MoO_3. The peaks at 2θ = 22.7 (001), 24.0 (110), 33.1 (111), 46.5 (002) are consistent with tetragonal WO_3 (JCPDS # 05-0388) with cell parameters a = 5.23 Å, b = 5.26 Å, c = 3.93 Å. The same characteristic peaks were also observed for MoO_3-WO_3 films prepared by atmospheric pressure chemical vapor deposition method [34,35].

X-ray photoelectron spectroscopy (XPS) measurements were employed to elucidate the elemental existence and oxidation states of W-Mo-O/rGO composites. The representative XPS survey spectra (Fig. S3) indicate the existence of molybdenum, tungsten, oxygen, and carbon elements. Fig. 5C

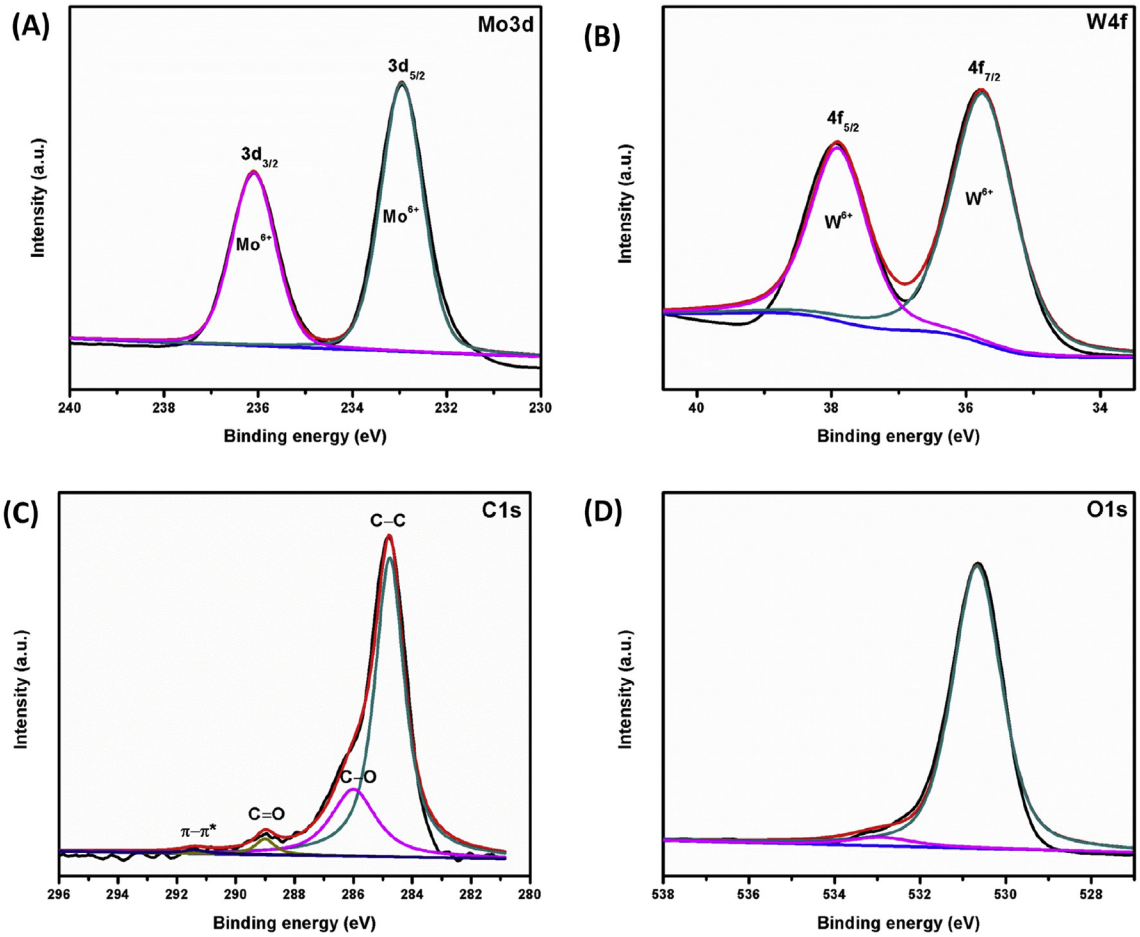

Fig. 5 – XPS spectra of W-Mo-O/rGO nanocomposite: Mo 3d orbital (A), W 4f orbital (B), C 1s orbital (C) O 1s orbital (D).

Please cite this article in press as: Imran M, et al., Tungsten-molybdenum oxide nanowires/reduced graphene oxide nanocomposite with enhanced and durable performance for electrocatalytic hydrogen evolution reaction, International Journal of Hydrogen Energy (2017), http://dx.doi.org/10.1016/j.ijhydene.2017.02.152

shows the high-resolution C1s XPS spectra which reveal the existence of four components corresponding to carbon atoms. The sharp peak at 284.6 eV may be attributed to C–C bonds of sp^2-hybridized graphitic structure and small intensity peaks at 286.7, 288.4 and 290.1 eV could be assigned to C–O bonds, carbonyl groups (C=O), and the $\pi-\pi^*$ [36]. After hydrothermal treatment, the intensities of all the peaks associated to oxygenated functional groups are sharply decreased, indicating the reduction of graphene oxide to rGO [37]. Fig. 5A shows high resolution XPS spectra of Mo 3d of as-prepared W-Mo-O/rGO. The Mo 3d spectrum exhibits peaks at 235.6 and 232.4 eV corresponding to spin orbit doublet and could be attributed to $3d_{3/2}$ and $3d_{5/2}$ of Mo cations (Mo^{6+}) with higher oxidation state [38]. XPS spectra of Mo 3d lack of lower oxidation states, confirming the existence of fully stoichiometric MoO_3, as reported previously [39]. The high resolution tungsten 4f XPS spectrum is shown in Fig. 5B for as synthesized mixed phase molybdenum-tungsten oxide and reduced graphene oxide composites. The W 4f profile can be fitted by two Gaussian peaks at 37.7 and 35.5 eV corresponding to the binding energy of electrons in the $4f_{5/2}$ and $4f_{7/2}$ levels of tungsten in higher oxidation state (W^{6+}) [40]. Without the observation of other lower valence states, WO_3 also possess a fully stoichiometric structure. The corresponding O 1s spectrum for W-Mo-O/rGO is shown in Fig. 5D. The O 1s spectrum is broad and asymmetric and can be deconvoluted into two peaks, the main component peak at 531.3 eV indicate the presence of lattice oxygen and oxygen in graphitic structure [41], while a small intensity peak at 533.1 eV may be assigned to surface adsorbed species [42,43].

We also measured Raman spectra of GO and W-Mo-O/rGO in the region from 1100 to 1800 cm^{-1} to detect the ordered and disordered crystalline structures of graphene. Fig. 4B shows the Raman spectrum of graphene oxide which exhibits well referred D band peak at about 1342 cm^{-1} due to breathing mode of k-point phonons of A_{1g} symmetry, and an another peak 1598 cm^{-1} which may be ascribed to G band, due to the doubly degenerated phonon mode of E_{2g} symmetry. Generally, the D band is attributed to the disorder and defects graphene layers, and the vibration of sp^2 carbon atoms is associated with the G band in a 2D hexagonal lattice. The ratio of intensities of D and G bands (I_D/I_G) is used to measure the change in graphene structure [44]. The I_D/I_G ratios of GO and W-Mo-O/rGO composite was calculated to be 1.14, which suggest a disorder in the GO and decrease in the sp^2 domains size due to the reduction of the exfoliated GO. In addition to the Raman spectroscopy, XPS spectra also confirm the reduction of oxygenated species on the O1s orbital which prevents the sheets from restacking together [45]. All these results confirm the reduction of graphene oxide (GO) to reduced graphene oxide (rGO) during the hydrothermal synthesis process for W-Mo-O/rGO composite.

To evaluate the electrocatalytic activities of W-Mo-O/rGO composites, 0.12 mg cm^{-2} sample was loaded on glassy-carbon electrode (GCE) and measured in 0.1 M $HClO_4$ under a three-electrode system. For comparison, tungsten-molybdenum oxide nanowires and commercial Pt/C (20 % wt) were also measured. Tungsten-molybdenum oxide nanowires exhibited inferior HER activity with an onset potential of about 160 mV. Impressively, W-Mo-O/rGO composites show highly efficient activity towards HER with the lowest onset potential of 50 mV. These results indicate that W-Mo-O alone is not an efficient HER catalyst and the synergistic effect between W-Mo-O nanowires and rGO play a key role for enhanced catalytic activity. It is documented that the presence of graphene oxide significantly improve the electrocatalytic HER performance. The deeper insight for synergistic enhancement into the electrocatalytic performance mechanism reveals that the structure of rGO consist folded 2D sheet, which can offer larger contact area and expose more active sites for HER [46] (see Table 1).

The linear sweep voltammograms (LSV) measured for commercial Pt/C is also provided, which showed an onset potential of ~0 V vs. RHE suggesting the validity of experimental conditions [47] (Fig. 6A). A Tafel slope, which determine the rate-determining step was also drawn to elucidate the HER mechanism [48–50]. It has been observed in previous studies that a Tafel slope of 30 mV dec^{-1} suggested that the hydrogen evolution proceeds through Volmer–Tafel mechanism and re-combination is rate-limiting step while 40 mV dec^{-1} Tafel slope follows Volmer–Heyrovsky mechanism with electrochemical desorption as rate-limiting step. A multiple reaction pathway was also suggested in case of 120 mV dec^{-1} Tafel slope due to surface blockage of adsorbed hydrogen [51]. The Pt/C shows a Tafel slope at ~34 mV $decade^{-1}$ involving Volmer–Tafel mechanism which is in good agreement with the previous reports and supports the validity of our electrochemical measurements [45]. The W-Mo-O nanowires has Tafel slope of 108 mV $decade^{-1}$, while the nanowires composites with rGO displays a Tafel slope of 46 mV $decade^{-1}$ (Fig. 6B), suggesting W-Mo-O/rGO composite follows Volmer–Heyrovsky reaction mechanism, and Volmer-step may be the rate-limiting step [8].

The HER mechanism reflected in the Tafel slope comprises following three steps

$$\text{Volmer}: \quad H_3O^+ + e \leftrightarrow H^*_{ad} + H_2O \ (\text{discharge reaction}) \tag{1}$$

$$\text{Tafel}: \quad 2H^*_{ad} \leftrightarrow H_2 \ (\text{combination reaction}) \tag{2}$$

$$\text{Heyrovsky}: \quad H_3O^+ + e + H^*_{ad} \leftrightarrow H_2 + H_2O \ (\text{ion} + \text{atom reaction}) \tag{3}$$

Previous reports suggested that reduced graphene oxide act as 2D support matrix for enhance catalytic activities as

Table 1 – Electrochemical HER comparison with reported materials.

Samples	Onset potential (mV vs. RHE)	Tafel slope (mV/dec)	Reference
W-Mo-O/rGO	50	46	Our study
MoO_2/rGO composite	190	49.2	[7]
MoP nanosheets	100	56.4	[25]
MoC NPs	120	62.6	[53]
m-MoO_{3-x}	140	56	[38]
WO_3 Nanoplates	90	101	[23]
MoO_3-MoS_2 nanowires	200	60	[54]
P-WN/rGO	46	54	[30]
MoS_2/N-MWCNTs	90	40	[55]
WS_2/SNCF	96	66	[56]

Please cite this article in press as: Imran M, et al., Tungsten-molybdenum oxide nanowires/reduced graphene oxide nanocomposite with enhanced and durable performance for electrocatalytic hydrogen evolution reaction, International Journal of Hydrogen Energy (2017), http://dx.doi.org/10.1016/j.ijhydene.2017.02.152

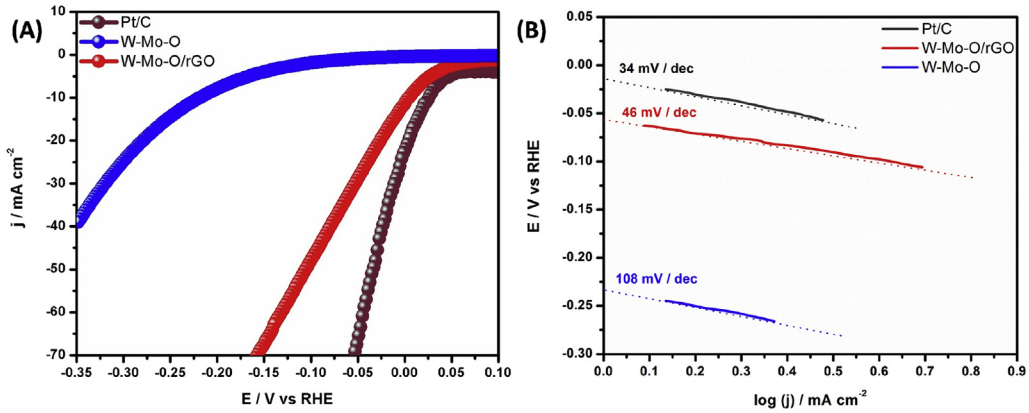

Fig. 6 – LSV curves in 0.1 M $HClO_4$ for W-Mo-O nanowires and W-Mo-O/rGO nanocomposite and commercial (20 wt %) Pt/C (A), Tafel plots of W-Mo-O nanowires and W-Mo-O/rGO nanocomposite and commercial Pt/C (B).

the support improves the electrical conductivity and favors the charge transfer [10]. In our study, W-Mo-O/rGO composites also showed enhanced and durable HER performance as compared to the W-Mo-O nanowires. The combination of rGO and W-Mo-O nanowires facilitate the electron transfer as shown in tafel slope which plays a key role in improving the kinetics and HER activity. To further gain insight into the electrode kinetics and interface reactions of the catalysts in HER, we performed electrochemical impedance spectroscopy (EIS) [52]. The Nyquist plots for tungsten-molybdenum oxide nanowires and W-Mo-O/rGO composites are shown in Fig. 7. The ohmic series resistance (R_s) was fitted by the intercept of the semicircle on the real axis and the charge transfer resistance (R_{ct}) was assigned to the semicircle of the Nyquist plot in terms of the equivalent circuit model. The Nyquist plots of W-Mo-O/rGO composites showed a much smaller semicircle with the lowest R_{ct} (100 Ω) compared to the W-Mo-O nanowires (812 Ω). The electrochemical impedance spectroscopy (EIS) results showed that W-Mo-O/rGO composites exhibited much lower R_{ct} which corresponds to faster reaction rate due to the presence of reduced graphene oxide which facilitate the reaction.

The long-term stability of the catalyst is highly demanded for electrocatalytic HER, as the reaction occurs on the surface of the electrode. To probe the durability and comparison for long-term stability of the W-Mo-O/rGO composite and commercial Pt/C catalysts, the accelerated durability test was performed up to 2000 cycles by following the same HER measurement conditions. As shown in Fig. 8, the polarization curve for W-Mo-O/rGO composite slightly shifted towards negative potential after 2000 cycles. The catalyst experienced loss of 1.8% in its electrocatalytic HER performance that is almost negligible. Whereas, the ADTs of commercial (20 wt %) Pt/C (inset Fig. 8) exhibit significant loss in it's HER performance due to degradation of the catalyst.

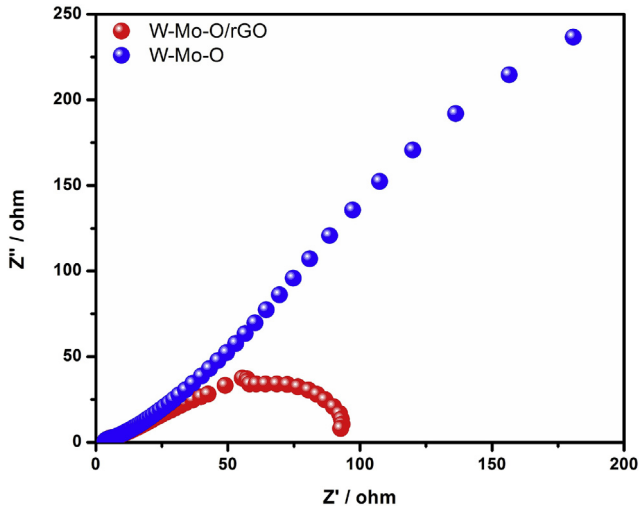

Fig. 7 – Nyquist plots of electrochemical impedance spectroscopy (EIS) for W-Mo-O nanowires and W-Mo-O/rGO composites.

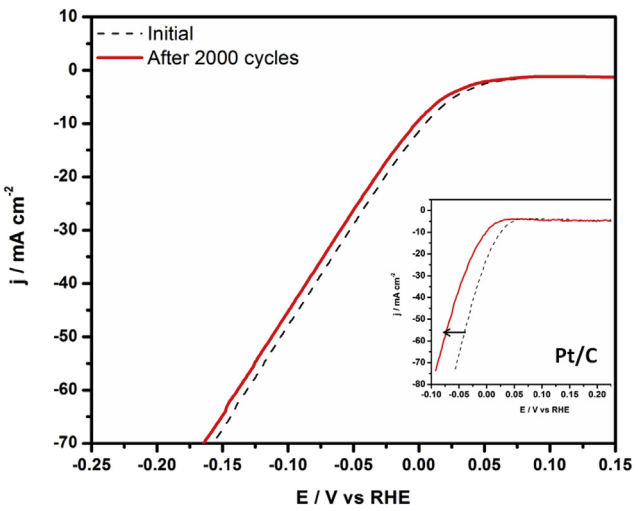

Fig. 8 – Accelerated durability test (ADTs) of HER performance for W-Mo-O/rGO composites up to 2000 cycles, inset: ADTs of commercial (20 wt %) Pt/C.

Please cite this article in press as: Imran M, et al., Tungsten-molybdenum oxide nanowires/reduced graphene oxide nanocomposite with enhanced and durable performance for electrocatalytic hydrogen evolution reaction, International Journal of Hydrogen Energy (2017), http://dx.doi.org/10.1016/j.ijhydene.2017.02.152

Conclusions

In this work, we have successfully synthesized W-Mo-O/rGO composites by a facile one step hydrothermal method and explored applications for enhanced and durable hydrogen evolution reaction (HER). Reduced graphene oxide as support provides strong interface interactions for anchoring tungsten-molybdenum oxide nanowires and this 3D network composites structure favors electron flow by providing synergistic effect. The resultant composite showed excellent electrocatalytic performance for hydrogen evolution reaction with onset potential of 50 mV, large cathodic currents and a Tafel slope of 46 mV decade^{-1} which are comparable with the commercial Pt/C. Moreover, the W-Mo-O/rGO composite showed a highly durable performance even up to 2000 cycles. The improved activity towards HER may also be attributed by mixed phase alloying of tungsten and molybdenum and highly conductive support with more active sites and synergistic effect between them. Therefore, the idea of alloying different metals and rGO as support works as highly active electrocatalysts for HER and provide a new route for the production of industrial scale, low-cost and environment friendly catalysts for hydrogen production.

Acknowledgement

The authors acknowledge financial support from CAS-TWAS President Fellowship programmes, USTC and Anhui Government Scholarship programmes.

Appendix A. Supplementary data

Supplementary data related to this article can be found at http://dx.doi.org/10.1016/j.ijhydene.2017.02.152.

REFERENCES

[1] Turner JA. Sustainable hydrogen production. Science 2004;305:972–4.
[2] Michael GW, Emily LW, James RM, Shannon WB, Qixi M, Elizabeth AS, et al. Solar water splitting cells. Chem Rev 2010;110:6446–73.
[3] Vojislav RS, Bongjin SM, Matthias A, Karl JJM, Christopher AL, Wang GF, et al. Trends in electrocatalysis on extended and nanoscale Pt-bimetallic alloy surfaces. Nat Mater 2007;6:241–7.
[4] Esposito DV, Hunt ST, Stottlemyer AL, Dobson KD, McCandless BE, Birkmire RW, et al. Low-cost hydrogen-evolution catalysts based on monolayer platinum on tungsten monocarbide substrates. Angew Chem Int Ed 2010;49:9859–62.
[5] Domínguez-Crespo MA, Plata-Torres M, Torres-Huerta AM, Arce-Estrada EM, Hallen-Lopez JM. Kinetic study of hydrogen evolution reaction on Ni_{30} Mo_{70}, $Co_{30}Mo_{70}$, $Co_{30}Ni_{70}$ and $Co_{10}Ni_{20}Mo_{70}$ alloy electrodes. Mater Charact 2005;55:83–91.
[6] Yvonne P, Ludwig AK. Hydrogen evolution electrocatalysis on AgPd(111) alloys. Electrocatalysis 2011;2:192–9.
[7] Tang YJ, Gao MN, Liu CH, Li SL, Jiang HL, Lan YQ, et al. Porous molybdenum-based hybrid catalysts for highly efficient hydrogen evolution 2015;127:13120–4.
[8] Liao L, Wang S, Xiao JJ, Bian X, Zhang Y, Scanlon MD, et al. A nanoporous molybdenum carbide nanowire as an electrocatalyst for hydrogen evolution reaction. Energy Environ Sci 2014;7:387–92.
[9] Yan Y, Xia BY, Qi XY, Wang HB, Xu R, Wang JY, et al. Nano-tungsten carbide decorated graphene as co-catalysts for enhanced hydrogen evolution on molybdenum disulfide. Chem Commun 2013;49:4884–6.
[10] Li Y, Wang H, Xie L, Liang Y, Hong G, Dai H. MoS2 nanoparticles grown on graphene: an advanced catalyst for the hydrogen evolution reaction. J Am Chem Soc 2011;133:7296–9.
[11] Liao L, Zhu J, Bian X, Zhu L, Micheál DS, Hubert HG, et al. MoS_2 formed on mesoporous graphene as a highly active catalyst for hydrogen evolution. Adv Funct Mater 2013;23:5326–33.
[12] Eric JP, James RM, Carlos GR, Adam JB, Alex MW, Nathan SL, et al. Nanostructured nickel phosphide as an electrocatalyst for the hydrogen evolution reaction. J Am Chem Soc 2013;135:9267–70.
[13] Eric JP, Carlos GR, Christopher WR, Nathan SL, Raymond ES. Highly active electrocatalysis of the hydrogen evolution reaction by cobalt phosphide nanoparticles. Angew Chem Int Ed 2014;126:5531–4.
[14] Zou XX, Zhang Y. Noble metal-free hydrogen evolution catalysts for water splitting. Chem Soc Rev 2015;44:5148.
[15] Peter CKV, Brian S, Chorkendorff I. Recent development in hydrogen evolution reaction catalysts and their practical implementation. J Phys Chem Lett 2015;6:951–7.
[16] Duck HY, Suenghoon H, Jae YK, Jae YK, Hunmin P, Sun HC, et al. Highly active and stable hydrogen evolution electrocatalysts based on molybdenum compounds on carbon nanotube–graphene hybrid support. ACS Nano 2014;8:5164–73.
[17] Liang M, Louisa RLT, Valerio M, Cristina G, Boon SY. Efficient hydrogen evolution reaction catalyzed by molybdenum carbide and molybdenum nitride nanocatalysts synthesized *via* the urea glass route. J Mater Chem A 2015;3:8361–8.
[18] Wang HT, Tsai C, Kong DS, Chan K, Abild-Pedersen F, Nørskov JK, et al. Transition-metal doped edge sites in vertically aligned MoS_2 catalysts for enhanced hydrogen evolution. Nano Res 2015;8:566–75.
[19] Hao JH, Yang WS, Zhang Z, Tang J. Metal–organic frameworks derived $Co_xFe_{1-x}P$ nanocubes for electrochemical hydrogen evolution. Nanoscale 2015;7:11055–62.
[20] Mendoza-Garcia A, Zhu H, Yu Y, Li Q, Zhou L, Su D, et al. Controlled anisotropic growth of Co-Fe-P from Co-Fe-O nanoparticles. Angew Chem Int Ed 2015;54:9642–5.
[21] Miao JW, Xiao FX, Yang HB, Khoo SY, Chen JZ, Fan ZX, et al. Hierarchical Ni-Mo-S nanosheets on carbon fiber cloth: a flexible electrode for efficient hydrogen generation in neutral electrolyte. Sci Adv 2015;1:e1500259.
[22] Cao BF, Gabriel MV, Joerg CN, Radoslav RA, Peter GK. Mixed close-packed cobalt molybdenum nitrides as non-noble metal electrocatalysts for the hydrogen evolution reaction. J Am Chem Soc 2013;135:19186–92.
[23] Hu WH, Han GQ, Dong B, Liu CG. Facile synthesis of highly dispersed $WO_3 \cdot H_2O$ and WO_3Nanoplates for electrocatalytic hydrogen evolution. J Nanomater 2015:346086.
[24] Ma RG, Zhou Y, Chen YF, Li PX, Liu Q, Wang JC. Ultrafine molybdenum carbide nanoparticles composited with carbon as a highly active hydrogen-evolution electrocatalyst. Angew Chem Int Ed 2015;54:14723–7.

Please cite this article in press as: Imran M, et al., Tungsten-molybdenum oxide nanowires/reduced graphene oxide nanocomposite with enhanced and durable performance for electrocatalytic hydrogen evolution reaction, International Journal of Hydrogen Energy (2017), http://dx.doi.org/10.1016/j.ijhydene.2017.02.152

[25] Cui W, Cheng NY, Liu Q, Ge CJ, Abdullah MA, Sun XP. Mo_2C nanoparticles decorated graphitic carbon sheets: biopolymer-derived solid-state synthesis and application as an efficient electrocatalyst for hydrogen generation. ACS Catal 2014;4:2658–61.
[26] Hu CG, Dai LM. Carbon-based metal-free catalysts for electrocatalysis beyond the ORR. Angew Chem Int Ed 2016;19:11736–58.
[27] Xie AZ, Xuan NG, Ba K, Sun ZZ. Pristine graphene electrode in hydrogen evolution reaction. ACS Appl Mater Interfaces 2017;9:4643–8.
[28] Duan JJ, Chen S, Benjamin AC, Gunther GA, Qiao SZ. 3D WS_2 nanolayers@heteroatom-doped graphene films as hydrogen evolution catalyst electrodes. Adv Mater 2015;27:4234–41.
[29] Duan JJ, Chen S, Mietek J, Qiao SZ. Porous C_3N_4 nanolayers@N-graphene films as catalyst electrodes for highly efficient hydrogen evolution. ACS Nano 2015;9:931–40.
[30] Yan HJ, Tian CG, Wang L, Wu AP, Meng MC, Zhao L, et al. Phosphorus-modified tungsten nitride/reduced graphene oxide as a high-performance, non-noble-metal electrocatalyst for the hydrogen evolution reaction. Angew Chem Int Ed 2015;54:6325–9.
[31] He CY, Tao JZ. Synthesis of nanostructured clean surface molybdenum carbides on graphene sheets as efficient and stable hydrogen evolution reaction catalysts. Chem Commun 2015;51:8323–5.
[32] Xu Y, Yi R, Yuan B, Wu XF, Marco D, Lin QL, et al. High capacity MoO_2/graphite oxide composite anode for lithium-ion batteries. J Phys Chem Lett 2012;3:309–14.
[33] Hummers WS, Offeman RE. Preparation of graphitic oxide. J Am Chem Soc 1958;80. 1339–1339.
[34] Gesheva KA, Ivanova T, Marsen B, Cole B, Miller EL, Hamelmann F. Structural and surface analysis of Mo–W oxide films prepared by atmospheric pressure chemical vapor deposition. Surf Coat Technol 2007;201:9378–84.
[35] Gesheva KA, Ivanova T. A low-temperature atmospheric pressure CVD process for growing thin films of MoO_3 and MoO_3-WO_3 for electrochromic device applications. Chem Vap Depos 2006;12:231–8.
[36] Some S, Kim YM, Yoon YH, Yoo HJ, Lee S, Park YH, et al. High-quality reduced graphene oxide by a dual-function chemical reduction and healing process. Sci Rep 2013;3:1929.
[37] Surajit S, Seok-Man H, Pooja D, Eunhee H, Young HS, HeeJoun Y, et al. Dual functions of highly potent graphene derivative–poly-l-lysine composites to inhibit bacteria and support human cells. ACS Nano 2012;6:7151–61.
[38] Luo Z, Miao R, Huan TD, Mosa IM, Poyraz AS, Zhong W, et al. Mesoporous MoO3–x material as an efficient electrocatalyst for hydrogen evolution reactions. Adv Energy Mater 2016:1600528.
[39] Cheng H, Kamegawa T, Mori K, Yamashita H. Surfactant-free nonaqueous synthesis of plasmonic molybdenum oxide nanosheets with enhanced catalytic activity for hydrogen generation from ammonia borane under visible light. Angew Chem Int Ed 2014;53:2910–4.
[40] Wagner CD, Riggs WM, Davis LE, Moulder JF. Photoelectron spectroscopy. Eden Praire, M N: Perkin Elmer Corp.; 1979. p. 146.
[41] David OS, Graeme WW, Payne DJ, Atkinson GR, Egdell RG, Law DSL. Theoretical and experimental study of the electronic structures of $MoO_3$and MoO_2. J Phys Chem C 2010;114:4636–45.
[42] Luo Z, Altug SP, Kuo CH, Miao R, Meng YT, Chen SY, et al. Crystalline mixed phase (Anatase/Rutile) mesoporous titanium dioxides for visible light photocatalytic activity. Chem Mater 2015;27:6–17.
[43] Jolanta SM, Soline-de D, Vincent M, Sandrine Z, Lorena K, Emrick B, et al. Li-ion intercalation in thermal oxide thin films of MoO_3 as studied by XPS, RBS, and NRA. J Phys Chem C 2008;112:11050–8.
[44] Wang Z, Chen T, Chen WX, Chang K, Ma L, Huang GC, et al. CTAB-assisted synthesis of single-layer MoS_2–graphene composites as anode materials of Li-ion batteries. J Mater Chem A 2013;1:2202–10.
[45] Ma YW, Sun LY, Huang W, Zhang L, Zhao J, Fan QL, et al. Three-Dimensional nitrogen-doped carbon nanotubes/graphene structure used as a metal-free electrocatalyst for the oxygen reduction reaction. J Phys Chem C 2011;115:24592–7.
[46] Li X, Jiang YM, Jia LP, Wang CM. MoO2 nanoparticles on reduced graphene oxide/polyimide-carbon nanotube film as efficient hydrogen evolution electrocatalyst. J Power Sources 2016;304:146–54.
[47] Xu Y, Wu R, Zhang J, Shi Y, Zhang B. Anion-exchange synthesis of nanoporous FeP nanosheets as electrocatalysts for hydrogen evolution reaction. Chem Commun 2013;49:6656–8.
[48] Pentland N, Bockris JOM, Sheldon E. Hydrogen evolution reaction on copper, gold, molybdenum, palladium, rhodium, and iron. J Electrochem Soc 1957;104:182–94.
[49] Sheng WC, Hubert AG, Yang SH. Hydrogen oxidation and evolution reaction kinetics on platinum: acid vs alkaline electrolytes. J Electrochem Soc 2010;157:B1529–36.
[50] Conway BE, Tilak BV. Interfacial processes involving electrocatalytic evolution and oxidation of H_2, and the role of chemisorbed H. Electrochim Acta 2002;47:3571–94.
[51] Bockris JOM, Potter EC. The mechanism of the cathodic hydrogen evolution reaction. J Electrochem Soc 1952;99:169–86.
[52] Xing ZC, Liu Q, Abdullah MA, Sun XP. Closely interconnected network of molybdenum phosphide nanoparticles: a highly efficient electrocatalyst for generating hydrogen from water. Adv Mater 2014;26:5702–7.
[53] Zhou XL, Jiang J, Ding T, Zhang JJ, Pan B, Zuo J, et al. Fast colloidal synthesis of scalable Mo-rich hierarchical ultrathin $MoSe_{2-x}$ nanosheets for high-performance hydrogen evolution. Nanoscale 2014;6:11046–51.
[54] Chen ZB, Dustin C, Benjamin NR, Ezra C, Mahendra KS, Thomas FJ. Core–shell MoO_3–MoS_2 nanowires for hydrogen evolution: a functional design for electrocatalytic materials. Nano Lett 2011;11:4168–75.
[55] Daia XP, Dua KL, Lia ZZ, Suna H, Yanga Y, Zhang W, et al. Enhanced hydrogen evolution reaction on few–layer MoS_2nanosheets–coated functionalized carbon nanotubes. Int J Hydrogen Energy 2015;40:8877–88.
[56] Wang QF, Yanzhang RP, Rena XN, Zhu H, Zhang M, Du ML. Two-dimensional molybdenum disulfide and tungsten disulfide interleaved nanowalls constructed on silk cocoon-derived N-doped carbon fibers for hydrogen evolution reaction. Int J Hydrogen Energy 2016;41:21870–82.

Please cite this article in press as: Imran M, et al., Tungsten-molybdenum oxide nanowires/reduced graphene oxide nanocomposite with enhanced and durable performance for electrocatalytic hydrogen evolution reaction, International Journal of Hydrogen Energy (2017), http://dx.doi.org/10.1016/j.ijhydene.2017.02.152